Acoustical-phonon-assisted resonant magneto-tunnelling in double-barrier heterostructures

1996 J. Phys.: Condens. Matter 8 8595

(http://iopscience.iop.org/0953-8984/8/44/011)

J. Phys.: Condens. Matter **8** (1996) 8595–8605. Printed in the UK

Acoustical-phonon-assisted resonant magneto-tunnelling in double-barrier heterostructures

Ø Lund Bø† and Yu Galperin†‡

† Department of Physics, University of Oslo, PO Box 1048 Blindern, N-0316 Oslo, Norway
‡ A F Ioffe Physico-Technical Institute, 194021 St Petersburg, Russia

Received 22 April 1996

Abstract. Acoustical-phonon-assisted resonant magneto-tunnelling in a double-barrier heterostructure has been considered. The calculations have been carried out within the coherent tunnelling model where the tunnelling current is related to the intra-well electron Green function. The magneto-tunnelling device is shown to be a convenient tool to study electron–phonon interaction since the effective coupling factor increases with increasing magnetic field. Our numerical calculations as well as analytical results for several limiting cases demonstrate that both dc and differential conductance profiles are sensitive to the presence of non-equilibrium phonons, as well as to their frequency distribution. In particular, we believe that our results can be useful for detection and spectroscopy of non-equilibrium acoustical phonons.

Semiconductor double-barrier resonant tunnelling structures (DBRTSs) have been extensively studied since their initiation by Tsu and Esaki [1] and first observation of negative differential resistance by Sollner *et al* [2]. Many important characteristics of DBRTSs have been analysed, in particular dc properties, phonon-assisted tunnelling, and time dependent processes (for a review see e.g. [3]). An interesting feature of the various structures is *inelastic* resonant tunnelling due to the coupling of tunnelling electrons to phonons. This effect provides a way to investigate electron and phonon modes, as well as electron–phonon interaction in such structures.

Earlier work on the phonon-assisted tunnelling was mainly focused on coupling to LO phonons [4–11]. Acoustical-phonon-assisted resonant tunnelling in double- [12] and triple- [13] barrier structures has been discussed within the sequential tunnelling model.

In this work, we study acoustical-phonon-assisted resonant magneto-tunnelling theoretically using the coherent tunnelling model. The initial motivation is provided by the experiments of Ouali *et al* [14], who observed inelastic tunnelling induced by non-equilibrium acoustical phonons. In the above experiment, phonon replicas appearing in dc current–voltage curves are interpreted as resonant tunnelling via impurity levels in the quantum well assisted by non-equilibrium acoustical phonons. Here we focus on the magnetic-tunnelling in a DBRTS in a situation when a strong magnetic field is applied parallel to the tunnelling current (see figure 1). In such a configuration the tunnelling occurs via intra-well Landau levels, the I–V-curves being sensitive to the modification of the electronic wavefunctions and the energies by the magnetic field. As a result, magnetic field appears to be an important tool for sample characterization.

The main feature of the configuration in question, $\boldsymbol{B}\|\boldsymbol{I}$, is that the tunnelling problem is essentially one-dimensional. As a result, phonon-assisted resonant tunnelling manifests

0953-8984/96/448595+11$19.50

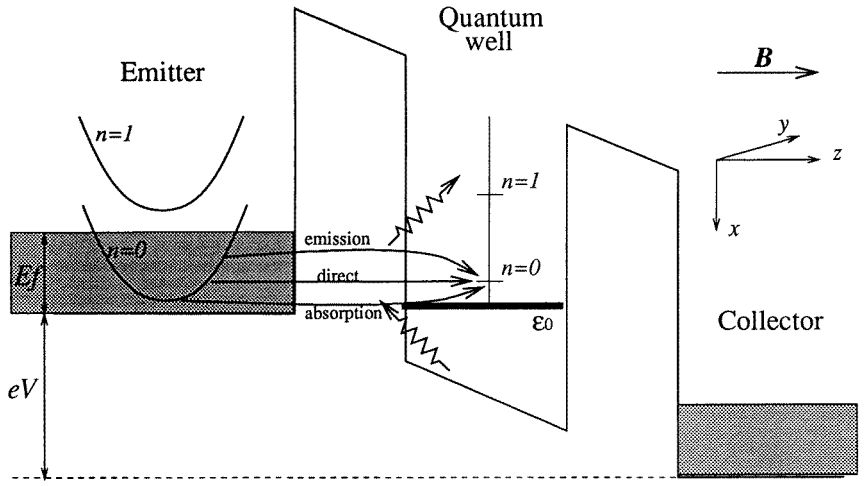

Figure 1. A schematic illustration of the DBRTS with the direct and inelastic resonant tunnelling processes.

itself in a clearer way which, in its turn, simplifies the problem of frequency-resolved phonon detection. In particular, one avoids the so-called electron recoil effect [15] tending to suppress and smear out the phonon replicas in the dc. Finally, it appears that the effective electron–phonon coupling increases with increasing magnetic field.

We consider the experimentally most extensively studied GaAs–AlGaAs heterostructures, having in mind for estimates a $GaAs^{+}$–$Al_{0.3}Ga_{0.7}As$–GaAs–$Al_{0.3}Ga_{0.7}As$–$GaAs^{+}$ DBRTS. In this case the barrier height is about 300 meV, and for the z-direction electron motion within the well one can assume that only one quasi-bound state with energy ϵ_0 exists. The zero reference energy is set to the bottom of the conduction band of the quantum well, and so the conduction band minimum of the emitter is in the symmetric case raised to $eV/2$ by the bias V, while the collector band edge is lowered to $-eV/2$. Under the magnetic field $\boldsymbol{B}\|\boldsymbol{I}\|\boldsymbol{z}$, the quasi-bound energy level ϵ_0 splits into a series of discrete Landau levels $\epsilon_0 + (n + \frac{1}{2})\hbar\omega_c$, where $\omega_c = eB/m^*$ is the cyclotron frequency. The electronic energy levels in the leads, on the other hand, form sets of Landau bands $eV/2 + \epsilon_z(k_{e,z}) + (n_e + \frac{1}{2})\hbar\omega_c$ and $-eV/2 + \epsilon_z(k_{c,z}) + (n_c + \frac{1}{2})\hbar\omega_c$, respectively, where $\epsilon_z(k_z) = \hbar^2 k_z^2/2m^*$ is the kinetic energy along the tunnelling direction. Here, the effective masses in the well and in the leads are assumed to be equal.

The quantum well electron wavefunction can be expressed as a product of a quasi-bound state $\chi(z)$ multiplied by the wavefunction corresponding to the in-plane $(x–y)$ motion. Under the Landau $\boldsymbol{A} = (0, Bx, 0)$ the wavefunctions can thus be specified by the set of quantum numbers $\alpha = (n, k_y)$ as

$$\phi_\alpha(\boldsymbol{r}) = (1/\sqrt{L_y})\exp(\mathrm{i}k_y y)\varphi_n(x + l^2 k_y)\chi(z)$$

with the corresponding energy levels (measured from the conduction band edge)

$$E_\alpha = E_n = \epsilon_0 + \hbar\omega_c(n + \tfrac{1}{2}).$$

Here $\varphi_n(x)$ denote harmonic oscillator eigenstates and $l \equiv \sqrt{h/eB}$ is the Landau magnetic length.

Similarly, electron states in the leads are specified by the quantum numbers $\beta = (m, k_{j,y}, k_{j,z})$, where $j \equiv e$ (c) refers to emitter (collector) states, respectively. The corresponding wavefunctions and energy levels under the bias eV are

$$\phi_{j,\beta}(\boldsymbol{r}) = (1/\sqrt{L_y L_z}) \exp(\mathrm{i}k_{j,z}z + \mathrm{i}k_{j,y}y)\varphi_m(x + l^2 k_{j,y})$$
$$E_{j,\beta} = [(\hbar k_{j,z})^2/2m^*] + \hbar\omega_c(m + \tfrac{1}{2}) + a_j eV$$

where in the symmetric case $a_e = \frac{1}{2}$ and $a_c = -\frac{1}{2}$.

Using this set of basic functions the model DBRTS is described with the Hamiltonian

$$\mathcal{H} = \mathcal{H}_e + \mathcal{H}_{ph} + \mathcal{H}_{e-ph}.$$

The electronic part of this Hamiltonian is given by

$$\mathcal{H}_e = \sum_{j,\beta} E_{j,\beta} c^\dagger_{j,\beta} c_{j,\beta} + \sum_{\alpha} E_\alpha c^\dagger_\alpha c_\alpha + \sum_{j,\alpha,\beta} [V_{j,\beta\alpha} c^\dagger_\alpha c_{j,\beta} + \mathrm{HC}]$$

where the tunnel matrix elements $V_{j,\beta\alpha}$ have in principle to be calculated using the eigenstates listed above according to Bardeen's prescription [16]. In our model, we ignore scattering due to interface roughness and impurities and the quantum numbers n and k_y are thus conserved during the tunnelling process. Consequently, the tunnelling matrix elements can be written

$$V_{j,\beta\alpha} = \delta_{m,n}\delta(k_y - k_{j,y}) V_{j,n}(k_{j,y}, k_{j,z}). \tag{1}$$

The phonon Hamiltonian is simply given by

$$\mathcal{H}_{ph} = \sum_{\boldsymbol{q}} \hbar\omega_{\boldsymbol{q}} b^\dagger_{\boldsymbol{q}} b_{\boldsymbol{q}}.$$

In the presence of an isotropic non-equilibrium acoustical phonon pulse, the total phonon distribution function $N(\hbar\omega_{\boldsymbol{q}})$ can be written

$$N(\hbar\omega_{\boldsymbol{q}}) = N_{eq}(\hbar\omega_{\boldsymbol{q}}) + N_{neq}(\hbar\omega_{\boldsymbol{q}})$$

where $N_{eq}(\hbar\omega_{\boldsymbol{q}}) = [\exp(\hbar\omega_{\boldsymbol{q}}/K_B T) - 1]^{-1}$ is the Planck distribution of equilibrium phonons, while $N_{neq}(\omega_{\boldsymbol{q}})$ is the occupation number of the non-equilibrium acoustical phonon pulse. One might however equally well apply the formulae to calculate the effects of a more general (possibly anisotropic) phonon distribution with the replacement $N(\hbar\omega_{\boldsymbol{q}}) \to N_{\boldsymbol{q}}$. We assume the phonon distributions to have a peak situated below the Debye energy $\hbar\omega_D$. Consequently, the acoustical phonons under discussion have a linear dispersion law, $\omega_{\boldsymbol{q}} = s|\boldsymbol{q}|$.

In the regime of resonant tunnelling the electrons reside in the well for a long time. Consequently, the electron–phonon interaction is most important inside the well [7]. The electron–phonon interaction Hamiltonian can thus be expressed as [17]

$$\mathcal{H}_{e-ph} = \sum_{\alpha,\alpha_1,\boldsymbol{q}} D_{\alpha\alpha_1}(\boldsymbol{q})(b_{\boldsymbol{q}} + b^\dagger_{-\boldsymbol{q}}) c^\dagger_{\alpha_q} c_\alpha$$

where

$$D_{\alpha\alpha_1}(\boldsymbol{q}) \equiv D\sqrt{\frac{\hbar\boldsymbol{q}^2}{2\rho V_0 \omega_{\boldsymbol{q}}}} \int \phi^*_{\alpha_1}(\boldsymbol{r})\, \mathrm{e}^{\mathrm{i}\boldsymbol{q}\cdot\boldsymbol{r}}\, \phi_\alpha(\boldsymbol{r})\, \mathrm{d}\boldsymbol{r} \tag{2}$$

D is the deformation potential, and ρ is the mass density. We assume the magnetic field to be strong enough ($\omega_c \gg \omega_{\boldsymbol{q}}$) to avoid inter-Landau-level transitions. Thus, we furthermore concentrate on the tunnelling via the lowest Landau level. In this case $\alpha = (0, k_y)$,

$\alpha_1 = (0, k_{1y} = k_y + q_y)$ and the squared matrix elements, $|D_{\alpha\alpha_1}(\boldsymbol{q})|^2$, can be calculated explicitly using the above quantum well wavefunctions. For a rectangular well

$$|D_{\alpha\alpha_1}(\boldsymbol{q})|^2_{n,n_1=0} = \frac{4\pi\hbar D^2}{V_0 L_y \rho s} \frac{|\boldsymbol{q}| \sin^2(q_z d/2) \exp[-(q_\parallel l/2)^2]}{(q_z d)^2[(q_z d/2\pi)^2 - 1]^2} \delta(k_y + q_y - k_{1y}) \tag{3}$$

where $q_\parallel \equiv \sqrt{q_x^2 + q_y^2}$.

According to the theory of coherent phonon-assisted resonant tunnelling [6, 7] the dc can be expressed through the so-called transmission Green function, which is a two-particle Green function with a proper arrangement of the incoming and outgoing quantum numbers and energy variables. The original theory was derived for a 1D DBRTS within the wide-band approximation. This derivation is in general insufficient for the 3D magneto-tunnelling problem because of the strong energy dependence of the density of states in the latter case. However the expression obtained in [6] can be easily generalized beyond the wide-band approximation, arriving at

$$I_{dc} = \frac{e}{\pi\hbar} \sum_{\alpha,\alpha_1} \int \mathrm{d}\varepsilon \, \mathrm{d}\varepsilon_1 K_{\alpha\alpha_1}(\varepsilon, \varepsilon_1)[f_e(\varepsilon)\gamma_e(n, \varepsilon)\gamma_c(n_1, \varepsilon_1) - f_c(\varepsilon)\gamma_c(n, \varepsilon)\gamma_e(n_1, \varepsilon_1)] \tag{4}$$

where

$$K_{\alpha\alpha_1}(\varepsilon, \varepsilon_1) = \int \frac{\mathrm{d}\tau \, \mathrm{d}t \, \mathrm{d}s}{2\pi\hbar^3} \, \mathrm{e}^{\mathrm{i}[(\varepsilon-\varepsilon_1)\tau + \varepsilon_1 t - \varepsilon s]/\hbar} \, \Theta(s)\Theta(t) \langle c_\alpha(\tau - s) c^\dagger_{\alpha_1}(\tau) c_{\alpha_1}(t) c^\dagger_\alpha(0) \rangle$$

is the energy domain *transmission Green function*. Since both leads are assumed to be in a state of local thermal equilibrium, $f_{e(c)}(\varepsilon)$ is simply the Fermi fuction of the emitter (collector)

$$f_j(\varepsilon) = [\mathrm{e}^{(\varepsilon - E_f - a_j eV)/k_B T} + 1]^{-1}.$$

Finally, $\gamma_{e(c)}(n, \varepsilon)$ is the escape rate from the quantum well Landau state n with the energy ε to the emitter (collector). Usually, the energy distance between the resonance level in the well and the tops of the barriers is much greater than the escape rate from the well, γ, in which case the tunnelling matrix elements (1) can be considered as smooth functions of the energy in comparison with the energy dependence of the density of states in the leads,

$$g_j(n, \varepsilon) \equiv \sum_{k_{j,z}} \delta(\varepsilon - E_{j,\beta}).$$

Thus the escape rates γ_j are expressed as $\gamma_j(n, \varepsilon) = 2\pi |V_j|^2 g_j(n, \varepsilon)$, and in the case of a 3D dissipation-free emitter

$$\gamma_j(\alpha, \varepsilon) = \frac{\Upsilon_j \theta(\varepsilon - a_j eV + \hbar\omega_c(n + \frac{1}{2}))}{\sqrt{\varepsilon - a_j eV + \hbar\omega_c(n + \frac{1}{2})}}$$

where Υ_j is a constant characterizing the tunnelling strength.

To lowest order in the electron–phonon coupling, the transmission Green function is given by

$$K_{\alpha\alpha_1}(\varepsilon, \varepsilon_1) = |G_R(n, \varepsilon)|^2 \Big\{ \delta_{\alpha,\alpha_1} \delta(\varepsilon - \varepsilon_1) + \frac{1}{2\pi} \sum_{\boldsymbol{q}} |D_{\alpha\alpha_1}(\boldsymbol{q})|^2 |G_R(n_1, \varepsilon_1)|^2 [1 + N(\varepsilon - \varepsilon_1)] B(\boldsymbol{q}, \varepsilon - \varepsilon_1) \Big\} \tag{5}$$

where $N(\varepsilon)$ is the actual phonon distribution function,

$$B(\boldsymbol{q}, \varepsilon) = -2\Im D_R(\boldsymbol{q}, \varepsilon) = 2\pi[\delta(\varepsilon - \hbar\omega_{\boldsymbol{q}}) - \delta(\varepsilon + \hbar\omega_{\boldsymbol{q}})]$$

is the phonon spectral function and

$$G_R(n,\varepsilon) = 1/[\varepsilon - E_n + \mathrm{i}\gamma(n,\varepsilon)/2 - \Sigma_R(n,\varepsilon)]$$

is the quantum well retarded electron Green function broadened by tunnelling to the leads by the total escape rate $\gamma(n,\varepsilon) = \gamma_e(n,\varepsilon) + \gamma_c(n,\varepsilon)$ and dressed by the phonon coupling self-energy

$$\Sigma_R(n,\varepsilon) = \sum_{\boldsymbol{q},\alpha_1} |D_{\alpha\alpha_1}(\boldsymbol{q})|^2 \left[\frac{1 + N(\hbar\omega_{\boldsymbol{q}})}{\varepsilon - \hbar\omega_{\boldsymbol{q}} - E_{n_1} + \mathrm{i}\gamma(n_1, \varepsilon - \hbar\omega_{\boldsymbol{q}})/2} + \frac{N(\hbar\omega_{\boldsymbol{q}})}{\varepsilon + \hbar\omega_{\boldsymbol{q}} - E_{n_1} + \mathrm{i}\gamma(n_1, \varepsilon + \hbar\omega_{\boldsymbol{q}})/2} \right].$$

Note that the self-energy and thus the dressed Green function depend on the quantum number n only (not on k_y).

For the problem of interest, inter-level scattering is ignored and the sum over k_y, α_1 and the ε_1 integral appearing in (4) can easily be performed analytically. While doing this, we assume $\epsilon_0 + \hbar\omega_c(n + \frac{1}{2}) - \hbar\omega_{\boldsymbol{q}} - E_F \gg k_B T$ and $eV \geqslant 0$ in which case only the first term in (4) contributes, so we arrive at

$$I_{dc} = \frac{e g_B}{\pi\hbar} \sum_n \int \mathrm{d}\varepsilon\, f_e(\varepsilon)\gamma_e(n,\varepsilon)|G_R(n,\varepsilon)|^2 \Big\{ \gamma_c(n,\varepsilon) + \int_0^\infty \mathrm{d}q_z\, \mathrm{d}q_\parallel\, f(n,q_z,q_\parallel)[(N(\hbar\omega_{\boldsymbol{q}}) + 1)\gamma_c(n,\varepsilon - \hbar\omega_{\boldsymbol{q}})|G_R(n,\varepsilon - \hbar\omega_{\boldsymbol{q}})|^2 + N(\hbar\omega_{\boldsymbol{q}})\gamma_c(n,\varepsilon + \hbar\omega_{\boldsymbol{q}})|G_R(n,\varepsilon + \hbar\omega_{\boldsymbol{q}})|^2] \Big\}. \tag{6}$$

Here $f(n,q_z,q_\parallel)$ is the electron–phonon coupling factor

$$f(q_z,q_\parallel,n) \equiv \frac{L_y V_0 q_\parallel}{4\pi^3} \int \mathrm{d}k_{1y} |D_{\alpha\alpha_1}(\boldsymbol{q})|^2. \tag{7}$$

Since $f(q_z,q_\parallel,n)$, $G_R(n,\varepsilon)$ and $\gamma_e(n,\varepsilon)$ are all independent of the wave factor k_y, the corresponding k_y summation in (4) results only in a magnetic degeneracy factor $g_B = L_x L_y/2\pi l^2$.

An 'effective electron–phonon coupling factor',

$$g_{eff}^2 \equiv \int_0^\infty \mathrm{d}q_z\, \mathrm{d}q_\parallel\, f(0,q_z,q_\parallel)$$

can be defined in the reasonable limit $l \gg d$ (corresponding to $q_\parallel \ll q_z$). For $n = 0$ it can be written as

$$g_{eff}^2 \sim \frac{\hbar D^2}{\pi^2 \rho s l^2 d^2} \int_0^\infty \mathrm{d}Q_\parallel\, \mathrm{d}Q_z\, \frac{\sin^2(Q_z/2) Q_z Q_\parallel \exp(-(Q_\parallel/2)^2)}{Q_z^2[(Q_z/2\pi)^2 - 1]^2}$$

where the new dimensionless variables $Q_z \equiv q_z d$ and $Q_\parallel \equiv q_\parallel l$ have been introduced. The integral does not depend on d or l. Consequently, $g_{eff}^2 \propto B$ which encourages our use of a strong magnetic field to enhance the weak acoustical phonon manifestations in the dc. Similarly, in the opposite limit $l \ll d$, we arrive at $g_{eff}^2 \propto B^{3/2}$.

Figure 2 shows the results in the case of the experimentally reasonable temperature $T = 4.2$ K in the leads. Here we assume that the non-equilibrium phonons also have a Planck distribution characterized by the effective temperature $T_{eff} = 30$ K. We assumed $D = 12$ eV [18], and $\hbar\omega_c = 30$ meV, that corresponds to $B \approx 16$ T. The Fermi level can be adjusted by the variation of impurity concentration in the leads. With the choice $E_F = 30$ meV $< \frac{3}{2}\hbar\omega_c$, we ensure that only the lowest Landau channel

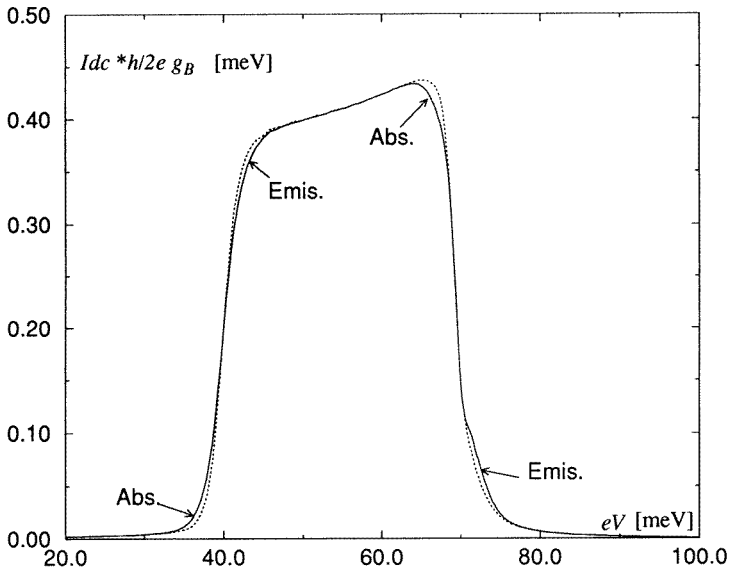

Figure 2. A static I–V-curve for a DBRTS with device parameters $\Upsilon_e = \Upsilon_c = 0.65$ (meV)$^{3/2}$, $\overline{h}\omega_c = 30$ meV, $\varepsilon_0 = 35$ meV, $E_F = 30$ meV, $d = 100$ Å, $s = 5000$ m s^{-1}, $\rho = 5.3$ g cm^{-3} and $D = 12$ eV. The curves obtained from equation (6) show results for $T = 4.2$ K in the absence of non-equilibrium phonons (dotted line) and in the presence of the non-equilibrium phonon pulse having a Planck distribution with $T_{eff} = 30$ K (solid line).

contributes. For the tunnelling strength, the symmetric and experimentally reasonable value $\Upsilon_e = \Upsilon_c = 0.65$ (meV)$^{3/2}$ was chosen. As shown by the arrows in the figure, phonon absorption (anti-Stokes) and phonon-stimulated emission (Stokes) replicas appear in the I–V-curve and are present at each side of both the rising and falling regions of the curve.

Assuming the temperature in the leads to be nearly unaffected by the non-equilibrium acoustical phonon pulse, we might concentrate on the rising region which has a couple of advantages due to the fact that the escape rates are smooth functions of energy. First, our formulae are simplified using the approximation

$$\gamma_j(n, \varepsilon \pm \overline{h}\omega_{\boldsymbol{q}}) \approx \gamma_j(n, \varepsilon) \tag{8}$$

which is justified provided $\overline{h}\omega_{\boldsymbol{q}} \sim k_B T_{eff} \ll E_F$. Second, in regions where the escape rates change abruptly, the charge redistribution effects are important and, in consequence, bistability of the I–V-curve may appear [4, 19]. Staying in the rising I–V-curve region where the escape rates are smooth functions of energy is thus an advantage if we want to avoid those effects. Within the approximation (8), equation (6) can be written as

$$I_{dc} = \frac{e g_B}{\pi \overline{h}} \sum_n \int \mathrm{d}\varepsilon \, f_e(\varepsilon) \frac{\gamma_e(n, \varepsilon)\gamma_c(n, \varepsilon)}{\gamma_e(n, \varepsilon) + \gamma_c(n, \varepsilon)} A(n, \varepsilon) \tag{9}$$

where $A(n, \varepsilon) \equiv 2\Im G_R(n, \varepsilon)$ is the spectral function of the quantum well electrons.

Figure 3(a) shows the dc in the rising-current region in the presence of a non-equilibrium acoustical phonon pulse when its background current is subtracted:

$$\Delta I_{dc}(N_{neq}) \equiv I_{dc}(N_{neq}) - I_{dc}(0).$$

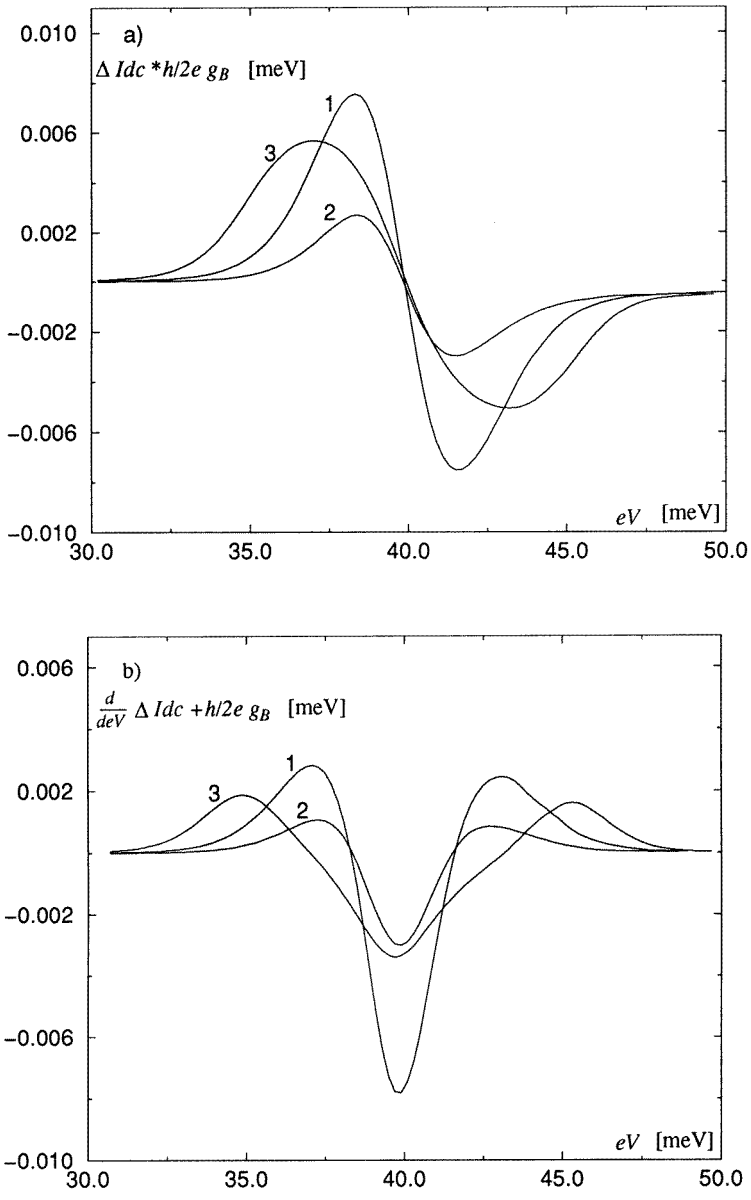

Figure 3. (a) The phonon-sensitive part of the current $\Delta I_{dc}(N_{neq})$ and (b) its voltage derivative $\partial\,\Delta I_{dc}/\partial(eV)$ for a DBRTS with parameters as in figure 2. The phonon-insensitive background is subtracted. The curves show results for non-equilibrium acoustical phonon pulses with different frequency distributions: a Planck distribution with $T_{eff} = 15$ K (curve 1) and 8 K (curve 2) and a Gaussian distribution centred at $\overline{h}\omega_0 = 2.5$ meV (curve 3). The structure on the left tails is due to phonon absorption while the right tails correspond to phonon emission.

The calculation was performed with the same device parameters and magnetic field as in figure 2. Two different Planck phonon distributions corresponding to $T_{eff} = 8$ and 15 K were considered, as well a Gaussian distribution centred near the frequency ω_0 (referred to

as 'monochromatic'),

$$N_{neq}(\overline{h}\omega_{\boldsymbol{q}}) = N_0 \exp\left[-\left(\frac{\omega_{\boldsymbol{q}} - \omega_0}{\delta\omega}\right)^2\right].$$

In the calculations, we used $N_0 = 200$, $\overline{h}\omega_0 = 2.5$ meV and $\overline{h}\delta\omega = 0.1$ meV. Also, the differential conductance $\mathrm{d}\,\Delta I_{dc}/\mathrm{d}(eV)$ has been plotted since it is closely related to the spectrum of the acoustical phonons (see the later analysis). The shape of the Stokes and anti-Stokes peaks in the dc and differential conductance curves clearly reflects the corresponding profile and strength of the frequency distribution of the non-equilibrium phonon pulse. We believe that a resonant double-barrier magneto-tunnelling structure can serve as a tool for a measurement of the latter.

Assuming thick barriers where $\gamma \ll \overline{h}\omega_{\boldsymbol{q}}$, the analytical analysis can be continued. In this case, to the lowest order in the electron–phonon interaction, the quantum well spectral function is approximated as a sum of three δ-functions with proper weight corresponding to the main peak, emission replica and absorption replica, respectively.

$$\begin{aligned} A(n,\varepsilon) \approx 2\pi\{&Z_m[n, N(\overline{h}\omega_{\boldsymbol{q}})]\delta(\varepsilon - E_n) + Z_e[n, N(\overline{h}\omega_{\boldsymbol{q}})]\delta(\varepsilon - E_n - \overline{h}\omega_{\boldsymbol{q}}) \\ &+ Z_a[n, N(\overline{h}\omega_{\boldsymbol{q}})]\delta(\varepsilon - E_n + \overline{h}\omega_{\boldsymbol{q}})\} \end{aligned} \tag{10}$$

where Z_m, Z_e and Z_a are the corresponding weight factors and are functionals of $N(\overline{h}\omega_{\boldsymbol{q}})$:

$$\begin{aligned} Z_m[n, N(\overline{h}\omega_{\boldsymbol{q}})] &\approx 1 - \int \mathrm{d}q_z\,\mathrm{d}q_\parallel\, f(n, q_z, q_\parallel)[1 + 2N(\overline{h}\omega_{\boldsymbol{q}})]/(\overline{h}\omega_{\boldsymbol{q}})^2 \\ Z_e[n, N(\overline{h}\omega_{\boldsymbol{q}})] &\approx \int \mathrm{d}q_z\,\mathrm{d}q_\parallel\, f(n, q_z, q_\parallel)[1 + N(\overline{h}\omega_{\boldsymbol{q}})]/(\overline{h}\omega_{\boldsymbol{q}})^2 \\ Z_a[n, N(\overline{h}\omega_{\boldsymbol{q}})] &\approx \int \mathrm{d}q_z\,\mathrm{d}q_\parallel\, f(n, q_z, q_\parallel)N(\overline{h}\omega_{\boldsymbol{q}})/(\overline{h}\omega_{\boldsymbol{q}})^2. \end{aligned}$$

With the substitution of (10) into (9), for the lowest Landau level, the dc can be expressed as

$$\begin{aligned} \Delta I_{dc}(eV, N_{neq}) = \frac{2eg_B}{\overline{h}}\frac{\gamma_e(eV)\gamma_c(eV)}{\gamma(eV)}\int \mathrm{d}q_z\,\mathrm{d}q_\parallel\,\frac{f(0, q_z, q_\parallel)N_{neq}(\overline{h}\omega_{\boldsymbol{q}})}{(\overline{h}\omega_{\boldsymbol{q}})^2}[&f_e(E_0 - \overline{h}\omega_{\boldsymbol{q}}) \\ &+ f_e(E_0 + \overline{h}\omega_{\boldsymbol{q}}) - 2f_e(E_0)] \end{aligned} \tag{11}$$

where ΔI_{dc} and $\gamma_j(\gamma_j(0, E_0) \to \gamma_j(eV))$ have now been written with the argument eV to emphasize their voltage dependence. In the particular limit of long phonon wavelengths, $\max(q_z d, Q_\parallel l) \ll 1$, the phonon coupling factor is dramatically simplified as

$$f(0, q_z, q_\parallel) \sim \frac{D^2\overline{h}}{4\pi^2\rho s}|\boldsymbol{q}|q_\parallel.$$

In the case of a Planck phonon distribution the above condition corresponds to $k_B T_{eff} \ll 2\overline{h}s/\max(l, d)$ and for a typical device with $\max(l, d) \sim 100$ Å it reads $T_{eff} \ll 10$ K.

Changing to polar coordinates $q_z \to |\boldsymbol{q}|\sin(\theta)$, $q_\parallel \to |\boldsymbol{q}|\cos(\theta)$, and to the new variable $\varepsilon \equiv \overline{h}s|\boldsymbol{q}|$, yields

$$\Delta I_{dc}(eV, N_{neq}) = \frac{eg_B D^2}{2\pi^2\rho\overline{h}^4 s^5}\frac{\gamma_e\gamma_c}{\gamma}\int \mathrm{d}\varepsilon\,\varepsilon N_{neq}(\varepsilon)[f_e(E_0 - \varepsilon) + f_e(E_0 + \varepsilon) - 2f_e(E_0)] \tag{12}$$

where $\gamma_{e(c)}$ is dependent on eV. Note that, in the discussed limit of long phonon wavelengths, the ratio $\Delta I_{dc}(N_{neq})/I_{dc}(0)$ is independent of the magnetic field, contrary to what one could naively expect from the B-dependence of the 'effective coupling factor'. The reason is that the $\boldsymbol{q}$ dependence of the integrand is in this limit mainly governed by

the occupation factor $N(\omega_q)$ (which is independent of B) and not by the electron–phonon coupling factor $f(n, q_z, q_\parallel)$.

Finally, we concentrate on the phonon absorption process responsible for the ΔI–V structure in the voltage regime $E_0 - E_F - eV/2 > 0$. Within this region of interest, the escape rates are nearly constant, and at zero temperature the differentiation of the Fermi functions with respect to eV just appears as delta functions. Thus the integral in (9) is easily performed and we arrive at a simple relation between the phonon distribution function and the differential conductance

$$N_{neq}(E_0 - E_F - eV/2) = \frac{2\pi^2\rho\hbar^4 s^5}{eD^2 g_B}\frac{\gamma}{\gamma_e\gamma_e}\frac{1}{E_0 - E_F - eV/2}\frac{\partial[\Delta I_{dc}(eV)]}{\partial(eV)}.$$

In the above considerations, we have concentrated on the rising-current region to take advantage of the smooth escape rates. However, for different reasons one could want to stay away from this region. Indeed, in that region the current structure is governed by an interplay between the resonant level in the well and the Fermi edge of the emitter, and a smearing of the Fermi function is important. The non-equilibrium acoustical phonon pulse could possibly heat the leads during the measurements, and so the smearing of Fermi functions would disturb the results. Alternatively, maybe we want to study also the *equilibrium* phonons with a focus on the *temperture* dependence of the Stokes and anti-Stokes peaks.

The smearing effects in the device considered so far can be avoided by a study of the falling-dc region. For this purpose it seems however better to use a 2D emitter device where the structure of phonon-assisted tunnelling is more pronounced. In this case the resonant tunnelling current is determined by the interplay between the resonant Landau level in the quantum well and the corresponding Landau level in the emitter. It is important that the latter can be kept at a sufficient distance from the Fermi edge. We should however remember that we are now in a region where the escape rates are no longer smooth functions of energy. Consequently, we should be aware of charge redistribution effects responsible for bistability in the I–V curves.

Figure 4 shows a calculation with a semi-elliptic density-of-states profile of the 2D emitter [20]

$$\gamma_e(n, \varepsilon) = \Upsilon_e\frac{4\hbar}{\sqrt{2m^*}L_{ez}\nu}\sqrt{1 - \left(\frac{\varepsilon - E_{e,n}}{\nu}\right)^2}$$

where $E_{e,n} = eV/2 + \omega_c(n + \frac{1}{2}) + \varepsilon_e$, ε_e is the emitter quasi-bound level and L_{ex} is the width of the 2D emitter. The broadening ν of the electronic states in the lead depends on the magnetic field and is given by the expression $\nu \sim \sqrt{2\hbar^2 e\omega_c/\pi m^*\mu}$, where μ is the mobility of the 2DEG. In our example, $\mu \sim 10^6$ cm^2 V^{-1} s^{-1} and at $\hbar\omega_c = 30$ meV we obtain $\nu \sim 0.6$ meV. The calculation shows results for a Planck phonon distribution $N(\hbar\omega_q)$ for two different temperatures as calculated from (6). In the case of non-equilibrium phonons, the calculated $\Delta I_{dc}(T) \equiv I_{dc}(T) - I_{dc}(0)$ corresponds to what we earlier denoted as $\Delta I_{dc}(N_{neq})$ with the replacement $T_{eff} \to T$. In the case of equilibrium phonons, T denotes the real temperature and so we have to compare dc profiles at different temperatures to extract the information we want.

It is obvious that our device can also be used for phonon generation in addition to the phonon detection studied so far. We assume that every electron taking part in the inelastic spontaneous emission transport emits one phonon with a frequency distribution governed by $f(n, q_z, q_\parallel)$. As a result, the generation rate R can be determined as $R = I_{se}/e$, where I_{se}/e is the emission contribution to the tunnelling current at a given voltage V. The phonon

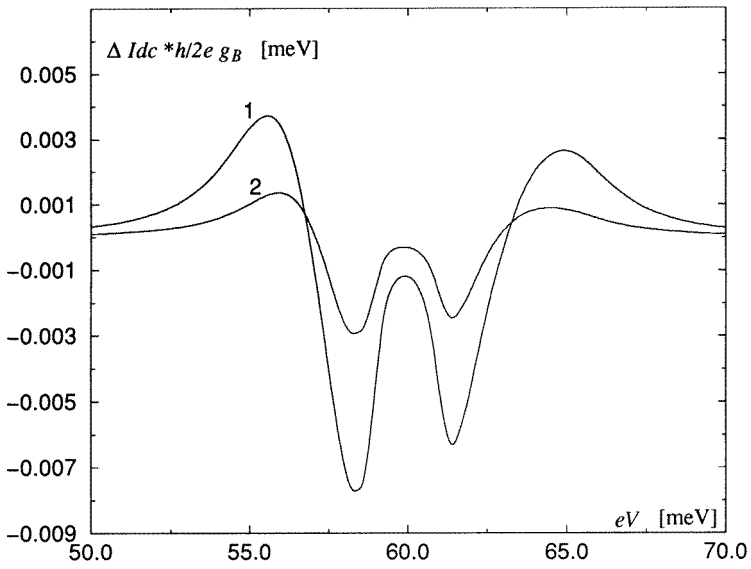

Figure 4. $\Delta I_{dc}(T)$ for a symmetric 2D emitter DBRTS with $\Upsilon_e = \Upsilon_c = 0.65$ (meV)$^{3/2}$, $\hbar\omega_c = 30$ meV, $\varepsilon_0 = 35$ meV, $E_F = 30$ meV $\epsilon_e = 5$ meV and $\nu = 0.6$ meV. The acoustical phonons have a Planck distribution, $T = 15$ K (curve 1) and 8 K (curve 2). The structure on the left tails is due to phonon absorption while the right tails correspond to phonon emission.

generation rate is thus given by equation (6) as

$$R(eV) = \frac{g_B}{\pi\hbar}\sum_n \int \mathrm{d}\varepsilon\, f_e(\varepsilon)\gamma_e(n,\varepsilon)|G_R(n,\varepsilon)|^2 \times \int_0^\infty \mathrm{d}q_z\, \mathrm{d}q_\parallel\, f(n,q_z,q_\parallel)\gamma_c(n,\varepsilon-\omega_{\boldsymbol{q}})|G_R(n,\varepsilon-\omega_{\boldsymbol{q}})|^2.$$

The resulting curve calculated for a 3D emitter device has a shape similar to that in figure 2.

In conclusion, we have calculated the change in resonant tunnelling current produced by acoustical phonons within the coherent tunnelling model. A magnetic field applied parallel to the current is shown to enhance the effective electron–phonon coupling and consequently the strength of the phonon replicas increases. Our calculations clearly show how the frequency distribution of the phonon pulse is reflected in both the I–V-curve and differential conductance. The resonant magneto-tunnelling device seems thus to be a good candidate to be employed in the spectroscopy of non-equilibrium acoustical phonons.

Acknowledgment

The present work has partially been supported by the Norwegian Research Council, grant no 100267/410.

References

[1] Tsu R and Esaki L 1973 *Appl. Phys. Lett.* **22** 562
[2] Sollner T C L G, Goodhue W D, Tannenwald P E, Parker C D and Peck D D 1983 *Appl. Phys. Lett.* **43** 588

[3] Mizuta H and Tanoue T 1995 *The Physics and Applications of Resonant Tunnelling Diodes* (Cambridge: Cambridge University Press)
[4] Goldman V J, Tsui D C and Cunningham J 1987 *Phys. Rev. Lett.* **58** 1256; *Phys. Rev.* B **36** 7635
[5] Glazman L I, Shekhter R I 1988 *Zh. Eksp. Teor. Fiz.* **94** 292 (Engl. Transl. 1988 *Sov. Phys.–JETP* **67** 163)
[6] Wingreen N S, Jacobsen K W and Wilkins J W 1988 *Phys. Rev. Lett.* **61** 1396
Wingreen N S, Jacobsen K W and Wilkins J W 1989 *Phys. Rev.* B **40** 11 834
[7] Jonson M 1989 *Phys. Rev.* B **39** 5924
[8] Cai W, Zheng T F, Hu P, Yudanin B and Lax M 1989 *Phys. Rev. Lett.* **63** 418
[9] Sokolovski D 1988 *Phys. Rev.* B **37** 4201
[10] Johansson P 1990 *Phys. Rev.* B **41** 9892
[11] Leadbeater M L, Alves E S, Eaves L, Henini M, Hughes O H, Celeste A, Portal J C, Hill G and Pate M A 1989 *Phys. Rev.* B **39** 3438
[12] Chevoir F and Vinter B 1989 *Appl. Phys. Lett.* **55** 1859
[13] Kozub V I and Rubin A M 1994 *Phys. Rev.* B **49** 5710
[14] Ouali F F, Zinov'ev N N, Challis L J, Sheard M, Henini M, Steenson D P and Strickland K R 1995 *Phys. Rev. Lett.* **75** 308
[15] Zou N and Chao K A 1992 *Phys. Rev. Lett.* **69** 3224
[16] Bardeen J 1961 *Phys. Rev. Lett.* **6** 57
[17] Mahan G D 1981 *Many Particle Physics* (New York: Plenum)
[18] Vinter B 1986 *Phys. Rev.* B **33** 5904
[19] Zou N, Willander M, Linnerud I, Hanke U, Chao K A and Galperin Y M 1994 *Phys. Rev.* B **49** 2193
[20] Ando T, Fowler A B and Stern F 1982 *Rev. Mod. Phys.* **54** 437